



HAL
open science

Filtered Asymmetrically Clipped Optical-OFDM with Index Modulation for Optical Wireless Systems

Ali Waqar Azim, Yannis Le Guennec, Marwa Chafii, Laurent Ros

► **To cite this version:**

Ali Waqar Azim, Yannis Le Guennec, Marwa Chafii, Laurent Ros. Filtered Asymmetrically Clipped Optical-OFDM with Index Modulation for Optical Wireless Systems. *IEEE Communications Letters*, 2021, 5 (5), pp.1592-1595. 10.1109/LCOMM.2020.3048894 . hal-03097509

HAL Id: hal-03097509

<https://hal.science/hal-03097509>

Submitted on 5 Jan 2021

HAL is a multi-disciplinary open access archive for the deposit and dissemination of scientific research documents, whether they are published or not. The documents may come from teaching and research institutions in France or abroad, or from public or private research centers.

L'archive ouverte pluridisciplinaire **HAL**, est destinée au dépôt et à la diffusion de documents scientifiques de niveau recherche, publiés ou non, émanant des établissements d'enseignement et de recherche français ou étrangers, des laboratoires publics ou privés.

Filtered Asymmetrically Clipped Optical-OFDM with Index Modulation for Optical Wireless Systems

Ali Waqar Azim, Yannis Le Guennec, Marwa Chafii, and Laurent Ros

Abstract—In this letter, we present filtered asymmetrically clipped optical-orthogonal frequency-division multiplexing with index modulation (FACO-OFDM-IM) for optical wireless systems. FACO-OFDM-IM optimizes the baseband bandwidth by filtering out-of-band spectral leakage caused by clipping. Additionally, IM enables FACO-OFDM-IM to impart granularity for spectral efficiency (SE)/energy efficiency (EE) trade-off and to achieve higher SE over established counterparts. Hereby, we elucidate the transceiver architecture, SE/EE trade-off, and bit-error-rate (BER). Simulation results establish that FACO-OFDM-IM attains higher spectral efficiencies than classical IM approaches and outperforms them for low alphabet cardinalities while marginally increasing the complexity.

Index Terms—Discrete Fourier transform, orthogonal frequency-division multiplexing, index modulation, intensity modulation and direct detection, optical wireless systems, Internet-of-Things.

I. INTRODUCTION

OPTICAL-orthogonal frequency-division multiplexing (O-OFDM) based on intensity-modulation and direct-detection optical wireless systems has been scrupulously examined in the literature. Among classical approaches, the scheme recognized for its energy efficiency (EE) is asymmetrically clipped O-OFDM (ACO-OFDM); which relies on clipping to attain non-negative signals [1]. However, clipping results in out-of-band harmonics culminating in the widening of baseband bandwidth (BB). To circumvent the aforesaid issue, [2] introduces filtered ACO-OFDM (FACO-OFDM), which filters the out-of-band clipping harmonics. So FACO-OFDM gain in spectral efficiency (SE) over ACO-OFDM depends on the bandwidth of the low-pass filter used to reject the clipping harmonics and its ability to preserve useful complex-valued sub-carriers. The maximum achievable SE gain can be up to 50%. At this point, it is important to highlight that ACO-OFDM and FACO-OFDM do not yield granularity for SE/EE trade-off as their spectral efficiencies vary only with change in \tilde{M} -quadrature-amplitude modulation (QAM) alphabet cardinality.

Inspired by the advantages and the SE/EE trade-off granularity capabilities of index modulation (IM) in radio-frequency systems, the amalgams of IM with O-OFDM have been examined in [3], [4], [5]. [3] explores ACO-OFDM-IM, which consolidates ACO-OFDM with IM, whilst, [5] explores its enhanced variant, AC enhanced O-OFDM-IM (ACEO-OFDM-IM) which employs M -pulse-amplitude modulation (PAM). It is accentuated that the BB of ACO-OFDM-IM and ACEO-OFDM-IM, in their original design, is not optimized, thus, by

extension, their spectral efficiencies are not optimal neither. In terms of SE, when $\tilde{M} = M^2$, we observe that (i) ACO-OFDM-IM achieves almost the same peak SE as that of ACO-OFDM and significantly less than the peak SE of FACO-OFDM; and (ii) ACEO-OFDM-IM attains significantly higher peak SE than ACO-OFDM and less SE than the peak SE of FACO-OFDM-IM. Nonetheless, the IM approaches are capable of providing granularity for SE/EE trade-off which is useful for applications requiring varying spectral and/or energy efficiencies, such as Internet-of-Things (IoT). To conclude, it is apparent that apart from SE/EE trade-off advantage, the usefulness of the IM approaches is rather questionable because the gain in SE over classical O-OFDM counterparts, such as FACO-OFDM is non-existent.

In this work, we propose to amalgamate FACO-OFDM with IM, proceeding in FACO-OFDM-IM. The objective is to overcome the limitations of classical IM approaches by achieving higher SE for FACO-OFDM-IM relative to FACO-OFDM while conserving the granularity for the SE/EE trade-off. We consider real-valued virtual sub-carriers rather than complex-valued sub-carriers to effectively improve the SE using IM [5]. Moreover, we also employ Pascal's triangle (PT) based index mapping and de-mapping to prevent sub-block partitioning [5]. To the best of our knowledge, this is the first time an IM variant of FACO-OFDM is studied. Simulation results shall reveal the following concrete improvements of FACO-OFDM-IM: (i) higher SE (especially compared to classic FACO-OFDM), (ii) an efficient granularity for SE/EE trade-off, and (iii) better bit-error-rate (BER) performance in both line-of-sight (LOS) and time-dispersive channels.

We organize the rest of the article as follows. Section II analyzes the system model, presents some insights into the classical benchmarks and explicates the transceiver architecture of FACO-OFDM-IM. Section III evaluates the system performance in terms of SE, SE/EE trade-off and BER. Section IV renders the conclusions.

II. SYSTEM DESCRIPTION AND TRANSCIEVER DESIGN

A. Baseband Bandwidth Requirements

The frequency-domain (FD) symbol comprising of N complex-valued sub-carriers over-sampled by factor L is $X[\sigma]$, where $\sigma \in \Omega = \llbracket -LN/2, LN/2 - 1 \rrbracket$. For $X[\sigma]$, only the odd complex-valued positive frequency sub-carriers having indices $\sigma^+ = 2\zeta - 1 \in \Omega^+ \in \llbracket 0, N/2 \rrbracket$ with $\zeta \in \llbracket 1, N/4 \rrbracket$ can be modulated to conform with the frame structure of ACO-OFDM, whilst the sub-carriers having negative frequencies $\sigma^- = -2\zeta + 1 \in \Omega^- = \llbracket -1, -N/2 \rrbracket$ are used for Hermitian symmetry (HS). The remaining sub-carriers with indices $\sigma \in \Omega \cap (\Omega^+ \cup \Omega^-)$ are null to incorporate over-sampling by a factor L . The inter-carrier spacing between even and odd complex-valued sub-carriers is $\Delta f = 1/T_s$, where T_s is the

Ali Waqar Azim is with CEA Leti, MINATEC, 38054, Grenoble (email: aliwaqarazim@gmail.com)

Yannis Le Guennec and Laurent Ros are with Université Grenoble Alpes, CNRS, Institute of Engineering, Grenoble INP, GIPSA-LAB, 38000 Grenoble, France (email: {yannis.le-guennec, laurent.ros}@grenoble-inp.fr).

Marwa Chafii is with ETIS, UMR 8051, CY Cergy Paris Université, ENSEA, CNRS, 95000 Cergy, France (email: marwa.chafii@ensea.fr)

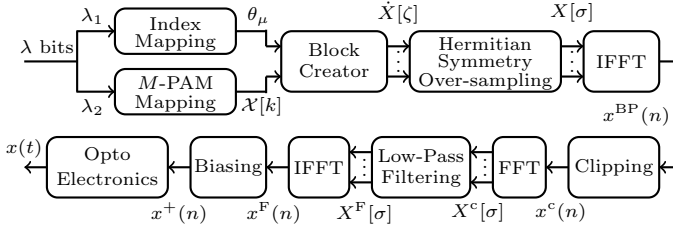


Fig. 1: Transmitter architecture for FACO-OFDM-IM.

time-domain (TD) symbol duration. As afore-mentioned, clipping leads to out-of-band harmonics for classical approaches, such as ACO-OFDM, ACO-OFDM-IM and ACEO-OFDM-IM. Hence the required BB is approximately $\tilde{B} \approx N/T_s$ [2]; which is twice the BB of bipolar real-valued pure frequency tones based signal, i.e., $N/2T_s$. Moreover, some out-of-band clipping distortion components may even fall on frequencies exceeding N/T_s . On the other hand, the BB of FACO-OFDM is $B = (N/2 + \alpha)/T_s$; which depends on the so-called tunability factor, α of the low-pass filter, where $\alpha \in \llbracket 0, (L-1)^{N/2} \rrbracket$.

B. Transceiver Design of FACO-OFDM-IM

The transmitter configuration of FACO-OFDM-IM is presented in Fig. 1. We have $N/2$ real-valued virtual sub-carriers (instead of $N/4$ complex-valued sub-carriers as in ACO-OFDM-IM) which are available for IM. Among these $N/2$ virtual sub-carriers, κ activated virtual sub-carriers are modulated with M -PAM alphabets. Thus, the total number of bits transmitted per symbol of duration T_s is

$$\lambda = \underbrace{\left\lfloor \log_2 \binom{N/2}{\kappa} \right\rfloor}_{:=\lambda_1} + \underbrace{\log_2(M^\kappa)}_{:=\lambda_2}, \quad (1)$$

where $\lfloor \cdot \rfloor$ is the floor function, and $\binom{\cdot}{\cdot}$ is the binomial coefficient.

The equiprobable bit sequence of length λ is split into λ_1 IM bits, and λ_2 constellation bits. An integer $Z \in \llbracket 0, 2^{\lambda_1} - 1 \rrbracket$ is generated using λ_1 ; which determines κ virtual sub-carriers to be activated using PT index mapping algorithm (cf. [5]); constituting the sub-carrier activation pattern (SAP), $\theta_\mu = \{\mu_1, \mu_2, \dots, \mu_\kappa\}$, where $\mu \in \llbracket 1, 2^{\lambda_1} \rrbracket$, $\mu_k \in \llbracket 1, N/2 \rrbracket$ with $k \in \llbracket 1, \kappa \rrbracket$. θ_μ is arranged in the descending order as $\mu_1 > \mu_2 > \dots > \mu_\kappa$. The complexity of index mapping can be reduced to $\mathcal{O}(0.5N)$ from $\mathcal{O}(0.25N^2)$ if PT based index mapping is used rather than combinatorial mapping. Using λ_2 , κ M -PAM alphabets, $\mathcal{X}[k]$ are generated; which modulate the real-valued virtual sub-carriers identified via θ_μ . Using θ_μ and $\mathcal{X}[k]$, we get $S[\mu_k]$ as

$$S[\mu_k] = \begin{cases} \sqrt{(1/2\kappa)}\mathcal{X}[k], & \mu_k \in \theta_\mu \\ 0, & \text{otherwise} \end{cases}. \quad (2)$$

Thereafter, using $S[\mu_k]$, we obtain $\dot{X}[\zeta] = S[\zeta] + jS[N/4 + \zeta]$, where $j^2 \triangleq -1$. By incorporating HS and consolidating over-sampling, the FD symbol is attained as

$$X[\sigma] = \begin{cases} \dot{X}[\zeta] & \sigma = \sigma^+ \in \Omega^+ \\ \dot{X}^*[\zeta] & \sigma = \sigma^- \in \Omega^- \\ 0 & \text{otherwise} \end{cases}, \quad (3)$$

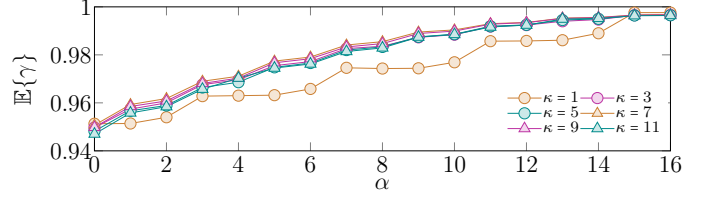


Fig. 2: The average reduction in symbol energy of $x^F(n)$ relative to $x^c(n)$ after low-pass filtering for different κ for $\{N, M, L\} = \{32, 2, 4\}$.

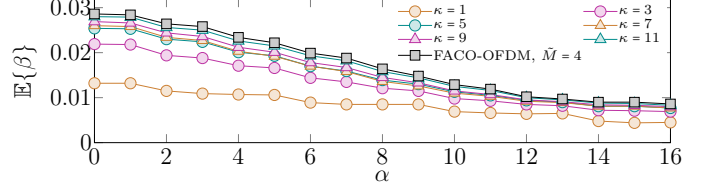


Fig. 3: The average bias required to attain non-negative signal for different κ when $N = 32$ and $L = 4$. We consider $M = 2$ for FACO-OFDM-IM and 4-QAM for FACO-OFDM.

where $(\cdot)^*$ denotes complex conjugate. Using LN -order inverse fast Fourier transform (IFFT), $X[\sigma]$ is transformed to a real-valued bipolar TD signal, $x^{\text{BP}}(n)$ with $n \in \llbracket 1, LN \rrbracket$; which adheres to the anti-symmetric property, i.e., $x^{\text{BP}}(l) = -x^{\text{BP}}(l + LN/2)$ with $l \in \llbracket 1, LN/2 \rrbracket$. Because of the scaling in (2), the average electrical symbol energy of $x^{\text{BP}}(n)$ is $\mathbb{E}\{|x^{\text{BP}}(n)|^2\} = \sum_n |x^{\text{BP}}(n)|^2 = 1$, where $\mathbb{E}\{\cdot\}$ evaluates the ensemble average. Zero level clipping of $x^{\text{BP}}(n)$ follows in a non-negative TD signal, $x^c(n)$ having an electrical symbol energy of $1/2$. It is highlighted that clipping of odd sub-carriers generates harmonic distortion only on unused even sub-carriers. It also culminates in significant out-of-band clipping harmonics resulting in spectral overflow. Thus, the BB of $x^c(n)$ is equal to \tilde{B} . To optimize the BB, LN -order FFT is applied to $x^c(n)$ to attain $X^c[\sigma]$, which is then passed through the low-pass filter $H^F[\sigma]$; which is a rectangular window with $H^F[\sigma] = 1$ for $\sigma \in \llbracket -N/2 - \alpha, N/2 + \alpha - 1 \rrbracket$ and zero otherwise, where $\alpha \in \llbracket 0, (L-1)^{N/2} \rrbracket$. For simplicity, in the sequel, we consider $\alpha \in \llbracket 0, N/2 \rrbracket$. The resulting FD symbol is $X^F[\sigma] = X^c[\sigma] \times H^F[\sigma]$. With the given parameters, the bandwidth of the low-pass filter is $B^F = (N + 2\alpha - 1)/T_s$; which results in a BB of $B = (N/2 + \alpha)/T_s$ for $X^F[\sigma]$. $X^F[\sigma]$ is then converted to the TD signal, $x^F(n)$ via LN -order IFFT. Low-pass filtering reduces the average electrical symbol energy of $x^F(n)$ relative to $x^c(n)$ by a factor γ , where the average electrical symbol energy of $x^F(n)$ is $\gamma(1/2)$. Here $\gamma = \sum_n |x^F(n)|^2 / \sum_n |x^c(n)|^2$ specifies the amount of signal energy retained after the low-pass filtering of out-of-band clipping harmonics. Fig. 2 illustrates the average γ for various κ . Observe that even with the highest clipping distortion rejection, i.e., $\alpha = 0$, 95% of the energy is yet retained in the un-filtered data implying that out-of-band clipping harmonics (in the band $(N/2T_s, N/T_s)$) contain minimal energy relative to the in-band information, i.e., $[0, N/2T_s]$.

The low-pass filtering also results in peak regrowth for the negative amplitude excursions of $x^F(n)$ (cf. [2]), therefore, a bias equal to $\beta = |\min x^F(n)|$ is added which results in $x^+(n) = x^F(n) + \beta$. The average bias required for different κ is illustrated in Fig. 3. We observe that the bias increases with

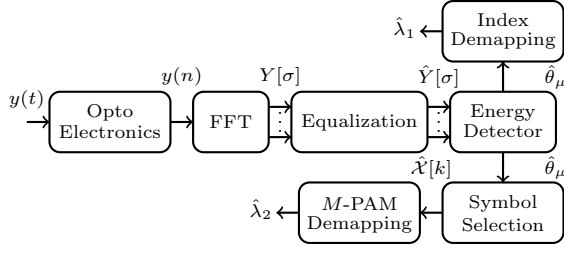


Fig. 4: Receiver architecture for FACO-OFDM-IM.

an increase in κ and decrease in α . It may also be noticed that FACO-OFDM requires the highest bias since all the odd complex-valued sub-carriers are used.

The average electrical symbol energy of $x^+(n)$ is scaled to unity, i.e., $E_{s(\text{elec})} = \mathbb{E}\{|x^+(n)|^2\} = 1$. After digital-to-analog conversion of $x^+(n)$, the intensity waveform $x(t) \geq 0$ is realized and is transmitted to the optical wireless channel.

The receiver architecture of FACO-OFDM-IM based on energy detector (ED) is presented in Fig. 4. After analog-to-digital conversion and LN -order FFT of the photo-detected intensity signal $y(t)$, we attain $Y[\sigma]$, which is then equalized using zero-forcing equalizer yielding $\hat{Y}[\sigma]$. The odd modulated complex-valued sub-carriers in $\hat{Y}[\sigma]$ are extracted as $\hat{Y}[\zeta] = 2\hat{Y}[2\zeta - 1]$, where the factor of 2 is used to counterbalance the halving of symbol amplitudes due to clipping. Next, we separate the real and imaginary components of $\hat{Y}[\zeta]$ as $\hat{Y}_{\Re}[\zeta] = \Re\{\hat{Y}[\zeta]\}$ and $\hat{Y}_{\Im}[\zeta] = \Im\{\hat{Y}[\zeta]\}$, where $\Re\{\cdot\}$ and $\Im\{\cdot\}$ respectively extract the real and imaginary components of a complex-valued number. Using $\hat{Y}_{\Re}[\zeta]$ and $\hat{Y}_{\Im}[\zeta]$, the $N/2$ virtual sub-carriers are obtained as $\hat{Y}[\mu_k] = [\hat{Y}_{\Re}[\zeta], \hat{Y}_{\Im}[\zeta]]^T$, where $[\cdot]^T$ is the transpose operator. It is recalled that κ among μ_k virtual sub-carriers are active, and under ideal circumstances, the energies of active virtual sub-carriers are higher than the inactive ones. Thus, to determine the active virtual sub-carriers, their energies are determined as $\xi_{\mu_k} = |\hat{Y}[\mu_k]|^2$. These energies are sorted in descending order and the κ highest energies are kept and the remaining $\mu_k - \kappa$ energies are discarded. The κ virtual sub-carriers are used to determine the SAP, $\hat{\theta}_\mu = \{\hat{\mu}_1, \hat{\mu}_2, \dots, \hat{\mu}_\kappa\}$; whose elements are sorted in descending order, such that $\hat{\mu}_1 > \hat{\mu}_2 > \dots > \hat{\mu}_\kappa$. $\hat{\theta}_\mu$ is then fed to the PT de-mapping algorithm to attain $\hat{\lambda}_1$ (cf. [5]). The κ M -PAM symbols on the active virtual sub-carriers are retrieved as $\hat{\mathcal{X}}[k] = \hat{Y}[\hat{\theta}_\mu]$, using which, $\hat{\lambda}_2$ is determined.

In terms of complexity, FACO-OFDM-IM transmitter requires additional LN -order FFT and LN -order IFFT, whilst the receiver requires the same number of FFTs as that of ACO-OFDM/ACO-OFDM-IM.

III. PERFORMANCE ANALYSIS OF FACO-OFDM-IM

A. Spectral Efficiency Analysis

For all the schemes, we consider N complex-valued sub-carriers and TD symbol duration of T_s . κ , $\tilde{\kappa}$ and $\tilde{\kappa}$ active virtual sub-carriers/complex-valued sub-carriers are respectively used for FACO-OFDM-IM, ACEO-OFDM-IM and ACO-OFDM-IM. It is recalled that the BB for ACO-OFDM, ACO-OFDM-IM, ACEO-OFDM-IM is \tilde{B} , whilst for FACO-OFDM and FACO-OFDM-IM, it is B . Accordingly, the spectral efficiencies of the above-mentioned schemes in bits/s/Hz are appraised to be $\eta^{\text{ACO}} = 0.25 \log_2(\tilde{M})$, $\eta^{\text{FACO}} =$

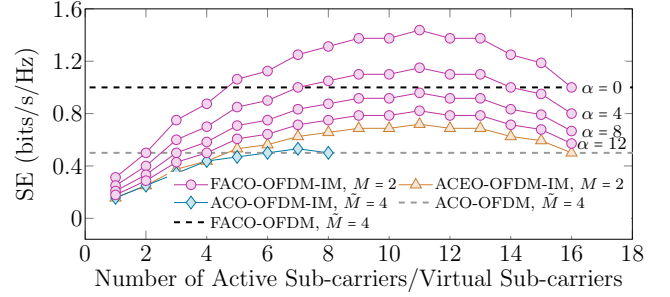


Fig. 5: The evolution of SE versus κ , $\tilde{\kappa}$ and $\tilde{\kappa}$ for FACO-OFDM-IM, ACEO-OFDM-IM and ACO-OFDM-IM, respectively for $N = 32$.

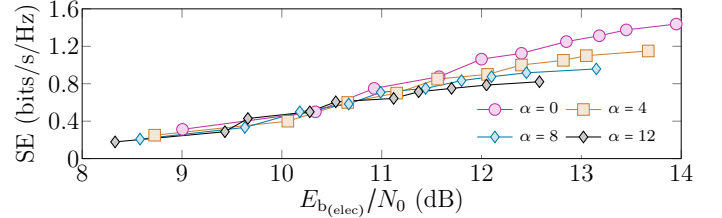


Fig. 6: SE/EE trade-off for FACO-OFDM-IM for different α using $\{N, M, L\} = \{32, 2, 4\}$ for BER of 10^{-3} .

$[N/4 \log_2(\tilde{M})]^{(N/2 + \alpha)^{-1}}$, $\eta^{\text{ACO-IM}} = [\lceil \log_2(\frac{N}{\tilde{\kappa}}) \rceil + \log_2(\tilde{M}^{\tilde{\kappa}})]N^{-1}$, $\eta^{\text{ACEO-IM}} = [\lceil \log_2(\frac{N}{\tilde{\kappa}}) \rceil + \log_2(\tilde{M}^{\tilde{\kappa}})]N^{-1}$ and $\eta^{\text{FACO-IM}} = [\lceil \log_2(\frac{N}{\tilde{\kappa}}) \rceil + \log_2(\tilde{M}^{\tilde{\kappa}})]^{(N/2 + \alpha)^{-1}}$. Note that $\alpha = 0$ results in the maximum SE for FACO-OFDM and FACO-OFDM-IM since the required BB is minimal. Fig. 5 illustrates the evolution of spectral efficiencies of ACO-OFDM-IM, ACEO-OFDM-IM and FACO-OFDM-IM (for different α) against $\tilde{\kappa}$, $\tilde{\kappa}$ and κ , respectively. Moreover, the spectral efficiencies of ACO-OFDM and FACO-OFDM (with $\alpha = 0$) are provided as benchmarks. We observe that the highest achievable SE of FACO-OFDM-IM for $\alpha \in \{0, 4\}$ and $M = 2$ is roughly 30% and 13% higher than that of FACO-OFDM. The gain in SE of FACO-OFDM-IM (with $M = 2$ and $\alpha = 0$) is around 65% over ACO-OFDM (using 4-QAM), 63% over ACO-OFDM-IM (using 4-QAM), and 50% over ACEO-OFDM-IM (using BPSK).

Owing to the log-concave nature of the binomial coefficient (cf. Fig. 5), it is possible to ascertain approximate κ , i.e., κ_{approx} which leads to maximum of achievable SE of FACO-OFDM-IM for a given N and M . To do so, we evaluate $d\lambda/d\kappa = 0$ [4], which results in

$$\kappa_{\text{approx}} \approx \left\lfloor \frac{MN}{2(M+1)} \right\rfloor. \quad (4)$$

B. Spectral-Energy Efficiency Performance Analysis

The EE is ascertained by evaluating the required signal-to-noise ratio per bit, $E_{b(\text{elec})}/N_0$ for a BER of 10^{-3} , where $E_{b(\text{elec})}/N_0 = E_{s(\text{elec})}T_s/(\lambda N_0)$, and N_0 is the mono-lateral noise spectral density. In Fig. 6, we evaluate SE/EE trade-off of FACO-OFDM-IM using sub-optimal low-complexity ED considering $\{N, M\} = \{32, 2\}$, $\kappa \in \llbracket 1, 11 \rrbracket$ and $\alpha \in \{0, 4, 8, 12\}$ for a target BER of 10^{-3} . The change in EE for different values of α is due to the fact that lower values of α require higher bias, however, its impact on EE is only marginal (cf. Fig. 6). We gather that the optimum

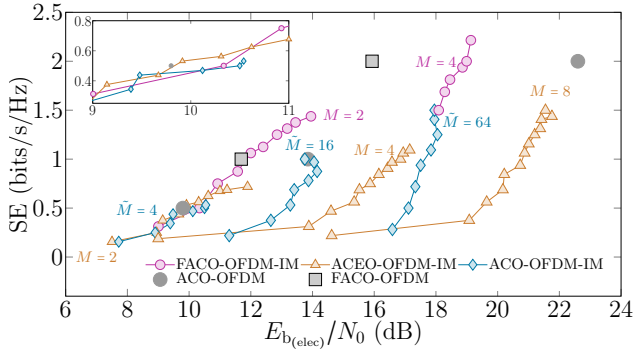


Fig. 7: SE/EE trade-off of FACO-OFDM-IM (with $\alpha = 0$) using $\{N, L\} = \{32, 4\}$ for BER of 10^{-3} .

value of α is zero because for this value, the filtering does not distort the in-band complex-valued sub-carriers nor their Hermitian symmetric counterparts while eliminating the out-of-band clipping harmonics to maximum extent with marginal impact on EE. The SE/EE trade-off comparison of the FACO-OFDM with classical counterparts is presented in Fig. 7 considering same target BER. We use ED based receiver for the IM approaches. For FACO-OFDM-IM, the SE between $[0.3125, 1.4375]$ bits/s/Hz is attained by varying $\kappa \in \llbracket 1, 11 \rrbracket$ and $\{M, \alpha\} = \{2, 0\}$, whilst the spectral efficiencies between $[1.5, 2.215]$ bits/s/Hz are realized for $\{M, \alpha\} = \{4, 0\}$ and varying $\kappa \in \llbracket 6, 11 \rrbracket$. We can observe that FACO-OFDM-IM is more energy-efficient than other counterparts. However, like other IM approaches, its EE drops for higher alphabet cardinalities implying that the region of interest (ROI) consists of spectral efficiencies attained using $\{M, \alpha\} = \{2, 0\}$. In the ROI, we observe the following concrete improvements of FACO-OFDM-IM over other counterparts: (i) highest peak achievable SE; (ii) it yields an extended granularity for SE/EE trade-off, which is not feasible with ACO-OFDM and FACO-OFDM; and (iii) it requires alphabets of lesser cardinality to achieve the same SE as that of counterparts.

C. Bit-Error-Rate Performance Analysis

The maximum achievable SE for FACO-OFDM-IM in ROI using $\{M, \kappa, \alpha\} = \{2, 11, 0\}$ is 1.4375 bits/s/Hz. We consider this as the reference SE to compare the BER performance of FACO-OFDM-IM with other counterparts. The results are illustrated in Fig. 8. We consider both the optimal maximum likelihood detector (MLD) and sub-optimal ED for FACO-OFDM-IM to illustrate the efficiency of ED. For ACO-OFDM and FACO-OFDM, the SE closest to the reference SE is 1.5 bits/s/Hz, which is, approximately 4% higher than the reference SE. Fig. 8(a) illustrates the BER performance in the LOS channel, while Fig. 8(b) portrays the BER performance in time-dispersive channel emulated using ceiling bounce model [6] with data-rate of 500 Mbits/s and delay spread of 10 ns. It is observed that FACO-OFDM-IM outperforms other alternatives in both LOS and time-dispersive channels; with MLD performing marginally better than ED. It is highlighted that ED sometimes obtains illegal index information which results in decoding errors, however, it can be ascertained from Fig. 8 that it is only with a marginal impact on BER. Unlike RF IM, where an intricate receiver design is mandatory for a

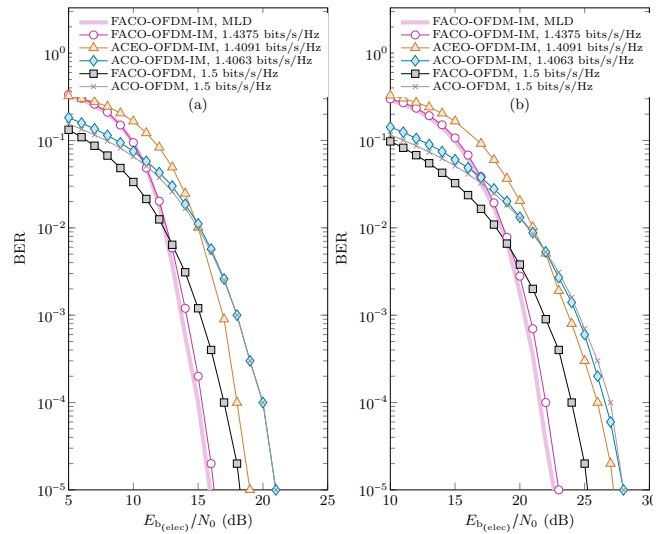


Fig. 8: BER performance comparison of FACO-OFDM-IM with classical counterparts for reference SE of 1.4375 bits/s/Hz in (a) LOS and (b) time-dispersive channel.

satisfactory performance, ED works nicely for FACO-OFDM-IM and thus does not require more sophisticated MLD (cf. Fig. 8). Furthermore, the complexity of MLD is $\mathcal{O}(2N^{-1}[2^{\lambda_1} M^\kappa + \kappa M])$ [5], which is significantly higher than that of ED's complexity, i.e., $\mathcal{O}(0.5N)$. The performance of FACO-OFDM-IM for the reference SE is better than classical approaches because of the following reasons: (i) it requires alphabets of lower cardinalities; (ii) it requires lesser bias than FACO-OFDM (cf. Fig. 3); and (iii) the signal structure of $X[\sigma]$ could be more sparse than ACO-OFDM, FACO-OFDM and ACO-OFDM-IM as not all the virtual sub-carriers are modulated.

IV. CONCLUSIONS

In this letter, we propose FACO-OFDM-IM which optimizes the BB requirement and employs IM. Consequently, it achieves higher spectral efficiencies relative to classical benchmarks. We establish that in addition to being superior in terms of SE and EE within the ROI, FACO-OFDM-IM also imparts granularity for SE/EE trade-off, which was lacking for classical O-OFDM counterparts. Furthermore, it outperforms other alternatives in terms of BER in both LOS and time-dispersive channels, and is energy-efficient for moderate spectral efficiencies in the ROI. We anticipate that the potentials of FACO-OFDM highlighted herein shall inspire further research, especially its operation with high alphabet cardinalities.

REFERENCES

- [1] J. Armstrong and A. J. Lower. Power efficient optical OFDM. *Electron. Lett.*, 42(6):370–372, 2006.
- [2] S. Mazahir, A. Chaaban, H. Elgala, and M.-S. Alouini. Achievable rates of multi-carrier modulation schemes for bandlimited IM/DD systems. *IEEE Trans. Wireless Commun.*, 18(3):1957–1973, 2019.
- [3] E. Başar and E. Panayırçı. Optical OFDM with index modulation for visible light communications. In *Intl. Wksp. Opt. Wireless Commun.*, pages 11–15, 2015.
- [4] A. W. Azim, M. Chafii, Y. Le Guennec, and L. Ros. Spectral and energy efficient fast-OFDM with index modulation for optical wireless systems. *IEEE Commun. Lett.*, 24(8):1771–1774, 2020.
- [5] A. W. Azim, Y. Le Guennec, M. Chafii, and L. Ros. Enhanced optical-OFDM with index and dual-mode modulation for optical wireless systems. *IEEE Access*, 8:128646–128664, 2020.
- [6] J. B. Carruthers and J. M. Kahn. Modeling of nondirected wireless infrared channels. *IEEE Trans. Commun.*, 45(10):1260–1268, 1997.